



## Review

Synthesis of LiCoO<sub>2</sub> thin films by sol/gel processH. Porthault<sup>a,b,\*</sup>, F. Le Cras<sup>a</sup>, S. Franger<sup>b</sup><sup>a</sup> CEA LITEN, 17 Rue des Martyrs, F-38054 Grenoble, France<sup>b</sup> Institut de Chimie Moléculaire et des Matériaux d'Orsay (ICMMO), UMR CNRS 8182, Université Paris XI, F-91405 Orsay, France

## ARTICLE INFO

## Article history:

Received 5 March 2010

Received in revised form 13 April 2010

Accepted 17 April 2010

Available online 24 April 2010

## Keywords:

LiCoO<sub>2</sub>

Thin films

Sol–gel process

Spin-coating method

## ABSTRACT

LiCoO<sub>2</sub> thin films were synthesized by sol/gel process using acrylic acid (AA) as chelating agent. The gel formulation was optimized by varying solvent (ethylene glycol or water) and precursors molar ratios (Li, Co, AA) in order to obtain a dense film for positive electrode of lithium batteries. The gel was deposited by spin-coating technique on an Au/TiO<sub>2</sub>/SiN/SiO<sub>2</sub>/Si substrate. Thin films were deposited by either single or multistep process to enhance the density of the thin film and then calcined during 5 h at 800 °C to obtain the *R-3m* phase (HT-LiCoO<sub>2</sub>).

A chemical characterization of the solution was realized by Fourier Transform Infrared (FTIR) spectroscopy. Thermal decomposition of precursors and gel was studied by Thermo Gravimetric Analyses (TGA). Further investigations were done to characterize rheologic behaviour of the gel and solvents affinity with the substrate. Crystallinity and morphology were analyzed respectively by X-ray diffraction (XRD) and Scanning Electron Microscopy (SEM).

The formation of *R-3m* phase was confirmed by the electrochemical behaviour of the gel derived LiCoO<sub>2</sub>. Cyclic voltammograms and galvanostatic cycling show typical curve shape of the HT-LiCoO<sub>2</sub>.

© 2010 Elsevier B.V. All rights reserved.

## Contents

1. Introduction .....	6262
2. Experimental .....	6262
3. Results and discussion .....	6264
4. Conclusions .....	6267
References .....	6267

## 1. Introduction

The considerable development of microelectronics and the miniaturization effort for the past two decades led to the development of microscale lithium-ion batteries. LiCoO<sub>2</sub> is a prime material as positive electrode for these batteries. Indeed, LiCoO<sub>2</sub> was intensively studied since 1980 [1] for its high specific energy (145 mAh g<sup>-1</sup>) and excellent cycle life [2–4]. Thin films of LiCoO<sub>2</sub> are currently mainly realized by plasma vacuum deposition method [5,6] but wet chemistry like sol/gel was also studied to synthesize this material [7–9]. Sol/gel process can be coupled with dip-coating [10] or spin-coating [11–14] methods to realize thin films. Acrylic acid was used in this study as chelating agent to limit drawbacks reported with other reactants, mainly pH

control during the gel formation and fluffiness during the heat treatment [8].

In this study, thin films of LiCoO<sub>2</sub> were deposited by spin-coating method using sol/gel process. An important part of this work was dedicated to the optimization of the formulation and the chemical characterization of the sol/gel process with Fourier Transform Infrared (FTIR) spectroscopy and X-ray diffraction (XRD) analyses. A peculiar concern was also to obtain high-density deposits.

The formation of the electrochemically active *R-3m* phase was checked by electrochemical analyses (cyclic voltammograms and galvanostatic cycling).

## 2. Experimental

LiCoO<sub>2</sub> material was synthesized by sol/gel process. Lithium acetate (Li(CH<sub>3</sub>CO<sub>2</sub>)·H<sub>2</sub>O, Fluka Analytical ≥99%) and cobalt acetate (Co(CH<sub>3</sub>CO<sub>2</sub>)<sub>2</sub>·4H<sub>2</sub>O, Fluka ≥99%) salts were dissolved in a solvent (distilled water (w) or ethylene glycol (EG) (Aldrich reagent Plus ≥99%)) and then mixed with acrylic acid (AA) (Aldrich ≥99%).

\* Corresponding author at: CEA LITEN, 17 Rue des Martyrs, F-38054 Grenoble, France. Tel.: +33 438782034; fax: +33 438785117.

E-mail address: [helene.porthault@cea.fr](mailto:helene.porthault@cea.fr) (H. Porthault).

Acrylic acid in this process acts as a chelating agent in order to obtain the gel. The molar ratio of Li:Co was varied from 1:1 to 1.06:1, whereas the molar ratio between the total metallic ions charges ( $M^+$ ) and acrylic acid ( $M^+ : AA$ ) varied from 1:0 to 1:1 (Table 1). The resultant solution was stirred at 75 °C during 24 h. In the case of water solvent, solutions were evaporated at 75 °C during several hours until a purple gel with desired viscosity was obtained (from 0.5 to 5 cP). For ethylene glycol solvent, desired viscosity was directly obtained by varying the overall concentration of the reactants in the initial composition.

Thin films were realized on a Si (1 0 0) wafer covered with 80 nm of  $SiO_2$  and 160 nm of SiN acting respectively as insulating and barrier films.  $TiO_2$  layer of 80 nm was used to improve the adhesion between the substrate and the current collector consisting in Au

**Table 1**Li:Co and  $M^+ : AA$  ratios of different solutions.

Gel	Li:Co	$M^+ : AA$	Solvent
A	1:1	1:1	EG
B	1:1	1:1	W
C	1.02:1	1:1	W
D	1.04:1	1:1	W
E	1.06:1	1:1	W
F	1.02:1	1:0.75	W
G	1.02:1	1:0.5	W
H	1.02:1	1:0.25	W
I	1.02:1	1:0	W

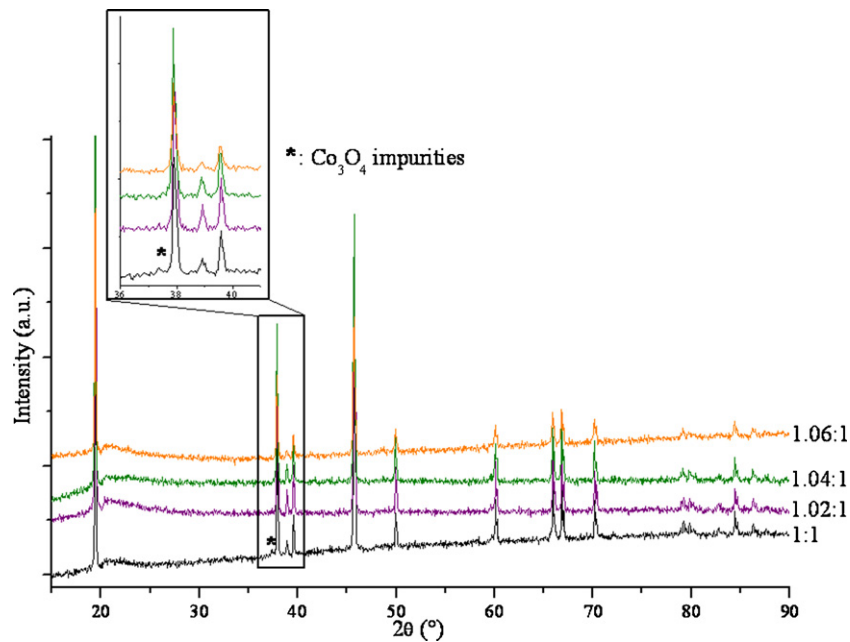
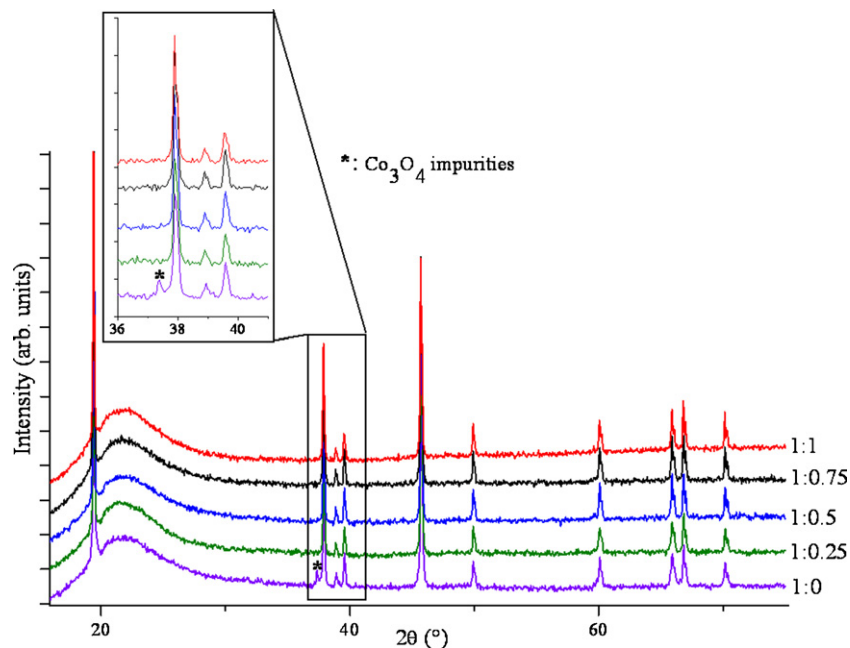
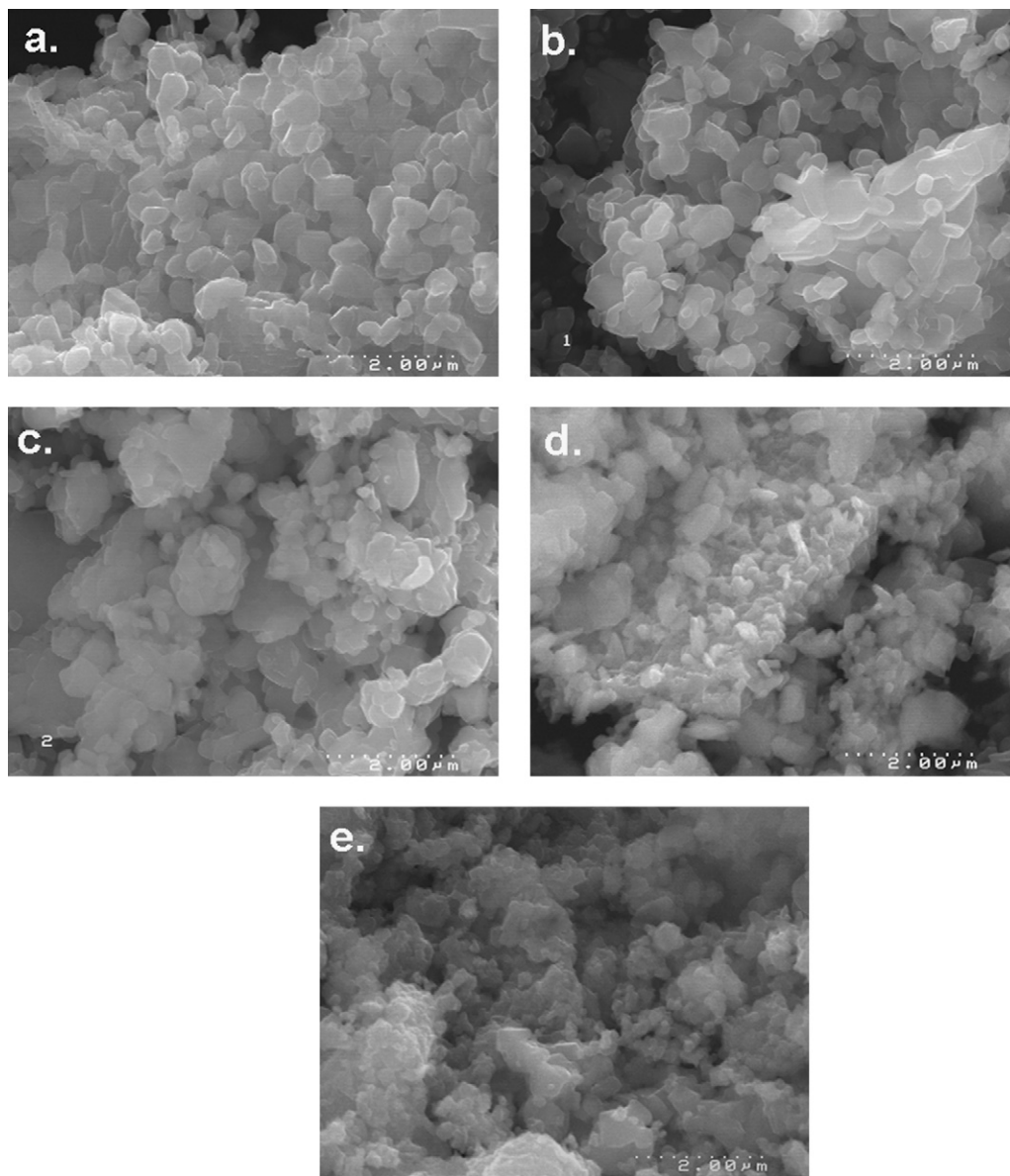


Fig. 1. XRD patterns of different Li:Co rates.

Fig. 2. XRD patterns of different  $M^+ : AA$  rates.



**Fig. 3.** SEM images of  $\text{LiCoO}_2$  powders calcined at  $800^\circ\text{C}$  ( $15,000\times$ ) (a) gel C, (b) gel F, (c) gel G, (d) gel H and (e) gel I.

layer of 400 nm. Monolayer thin films were realized by depositing the gel on this  $\text{Au/TiO}_2/\text{SiN/SiO}_2/\text{Si}$  substrate by spin coating at the speed of 2000 rpm during 40 s with an acceleration of 1000 rpm. Multilayer thin films were realized by repeating the previous process six times with a calcination between each deposit (calcination temperature was determined by TG analyses). These as-deposited films were then heat treated at  $800^\circ\text{C}$  during 5 h to obtain the desired  $R-3m$  phase ( $\text{HT-LiCoO}_2$ ).

Thermal decomposition of the gels was investigated by Thermo Gravimetric Analyses (TGA) with a SETSYS-1750-TG-DSC equipment. Fourier Transform Infrared (FTIR) spectra were acquired using a Thermo Nicolet FT-IR Nexus 870 spectrometer and a liquid cell with ZnSe crystal windows. Crystal structure of  $\text{LiCoO}_2$  was investigated on corresponding powders obtained after gel annealing at  $800^\circ\text{C}$ . Analyses were realized with a Brüker D8000 diffractometer using  $\text{Cu K}\alpha$  radiation. Morphology and surface aspects were observed with Scanning Electron Microscope (SEM) Hitachi 4000/4100. Gel viscosity was determined at room temperature by rheological measurements using an Anton Paar MCR 300 Series rheometer. Contact angles were measured with a Krüss DSA 10 system

at room temperature under controlled hygrometric conditions (80%).

Galvanostatic and cyclic voltammograms experiments were performed on coin cells. Lithium foils were used as anode material and a 1:1:3 mixture of ethylene carbonate (EC), propylene carbonate (PC) and dimethyl carbonate (DMC) containing 1 M of  $\text{LiPF}_6$  was used as electrolyte. The cathode consisted of composite electrode with 80 wt% of active material  $\text{LiCoO}_2$  powders synthesized by sol/gel, 10 wt% of polyvinylidene fluoride (PVDF, at 12 wt% in *n*-methylpyrrolidone (*n*-MP)) and 10 wt% of Super P Carbon, dispersed in *n*-MP. The obtained ink was coated on an aluminium foil and dried at  $50^\circ\text{C}$  during 24 h, coin cells were assembled in an argon-filled drybox. Cyclic voltammograms were carried out at  $5\ \mu\text{V s}^{-1}$  between 3 and 4.2 V (vs  $\text{Li/Li}^+$ ), galvanostatic cycling was done at a rate of C/5 between 3 and 4.2 V with a cell capacity of 350 mA h. All electrochemical tests were performed at  $20^\circ\text{C}$ .

### 3. Results and discussion

Samples with molar ratios of Li:Co in the range [1:1–1.06:1] were synthesized. The X-ray diffraction pattern of gel B reveals

the formation of  $\text{Co}_3\text{O}_4$  impurities (peak at  $2\theta = 37.4^\circ$ ) with stoichiometric ratios of Li:Co [1:1] due to lithium loss above  $750^\circ\text{C}$ . This evaporation is compensated when an excess of 2% of lithium is added (Fig. 1). Different molar ratios of  $\text{M}^+:\text{AA}$  were also tested to check the influence of the organic network formation on the final material. X-ray diffraction patterns show that except for the gel I (without chelating agent) where  $\text{Co}_3\text{O}_4$  impurities clearly appear, no differences are observed with the variation of  $\text{M}^+:\text{AA}$  ratios (Fig. 2). This is due to the final temperature of the heat treatment ( $800^\circ\text{C}$ ) which is sufficient to form  $\text{LiCoO}_2$  in any case. Scanning Electron micrographs realized on powders obtained by annealing the gel at  $800^\circ\text{C}$ , reveal an evolution of their morphology with the increase of acrylic acid concentration (Fig. 3). The grain morphology and size are more and more homogeneous when acrylic acid concentration increases. These results confirm the role of acrylic acid in the formation of organic network. A considerable organic network leads to a better repartition of metallic ions in the gel and inhibits particle growth in the early stages of the gel decomposition leading to a better homogeneity of the final material. Finally, a formulation with molar ratios of 1.02:1 for lithium to cobalt and 1:1 for total metallic charges ions to acrylic acid was found to lead the best characteristics considering composition and homogeneity aspects.

The formation of the interesting *R-3m* phase was checked by electrochemical experiments. Coin cells were realized using  $\text{LiCoO}_2$  powders obtained by annealing the gel described above at  $800^\circ\text{C}$  as active material. Cyclic voltammogram obtained is typical of *R-3m* phase which is characterized by three couple of well defined current peaks (Fig. 4). The first charge/discharge curves of gel derived  $\text{LiCoO}_2$  is presented in Fig. 5. Cell was charged from its rest potential to 4.2 V and then discharge to 3 V. The lithium concentration  $x$  is calculated from the current, the mass of active material and the elapsed time considering that all current is due to the insertion or extraction of lithium. The curve displays a wide potential plateau at 3.9 V and two smaller plateaus at higher potential. The first plateau is due to the expansion of the crystal network on the *c* direction. The two others plateaus correspond to the distortion of crystalline network from hexagonal to monoclinic [15]. Actually, the formation of *R-3m* phase by annealing the gel was confirmed by these electrochemical analyses.

FTIR analyses were carried out on precursors dissolved in water and gel B (Fig. 6). The two spectra of acetate salts are very similar. Indeed, salts dissolution in water inhibits the impact of metallic ions environment on acetate groups. In the spectrum of acrylic acid, the two peaks characteristic of the  $\text{C}=\text{C}$  double bond at 1233 and

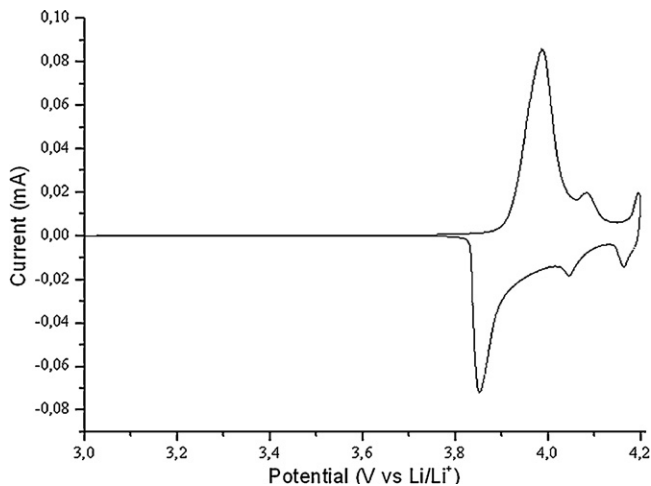


Fig. 4. Cyclic voltammogram of the gel derived  $\text{LiCoO}_2$  calcined at  $800^\circ\text{C}$  at a scan rate of  $5 \mu\text{V s}^{-1}$  at  $20^\circ\text{C}$ .

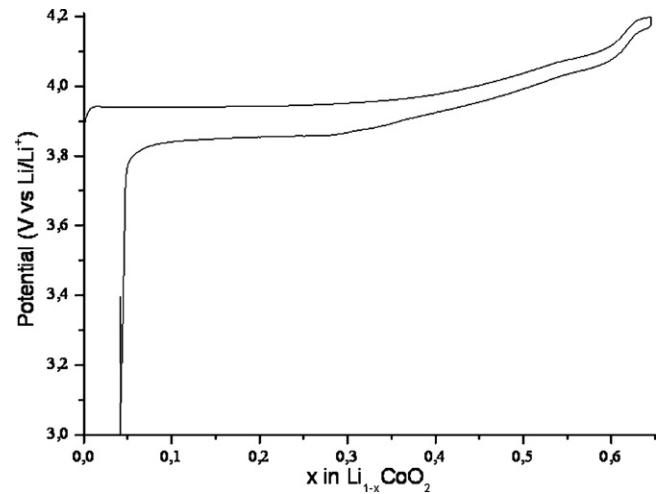


Fig. 5. First charge/discharge curves of gel derived  $\text{LiCoO}_2$  calcined at  $800^\circ\text{C}$  at a rate of C/5.

$1297 \text{ cm}^{-1}$  appear. Those peaks are less marked in the gel spectrum because of the appearance of a third peak at  $1277 \text{ cm}^{-1}$  which is associated to the opening of the  $\text{C}=\text{C}$  double bond to form the organic network. A second peak at  $1366 \text{ cm}^{-1}$  appears and reveals gel formation. Infrared spectra of gel at different steps of the process (before heating, after 24 h of heating and after evaporation) are presented in Fig. 7. The presence of the two peaks characteristic of the organic network formation at  $1277 \text{ cm}^{-1}$  and  $1366 \text{ cm}^{-1}$  before heating clearly shows that the formation of the gel begins as soon as precursors are mixed together. However, considering measurement conditions, these FT-IR analyses are only qualitative. Therefore, the impact of the heating step cannot be delinked from the reaction rate at room temperature.

The evolution of gels viscosity with the concentration variation was measured on gel A and gel B (Fig. 8). In the case of a water solvent (gel B), concentration varies with solvent evaporation (heating at  $75^\circ\text{C}$  during several hours). For the gels prepared with an ethylene glycol solvent (gel A), different overall concentration of reactants were achieved by varying the initial solvent amount. The concentration range attainable is limited by the dissolution of salts, the solubility limit in EG solvent was found at 15 wt% for lithium acetate and 38 wt% for cobalt acetate. These measurements reveal that it is easier to obtain high concentration and high density with ethylene glycol solvent due to the initial viscosity of

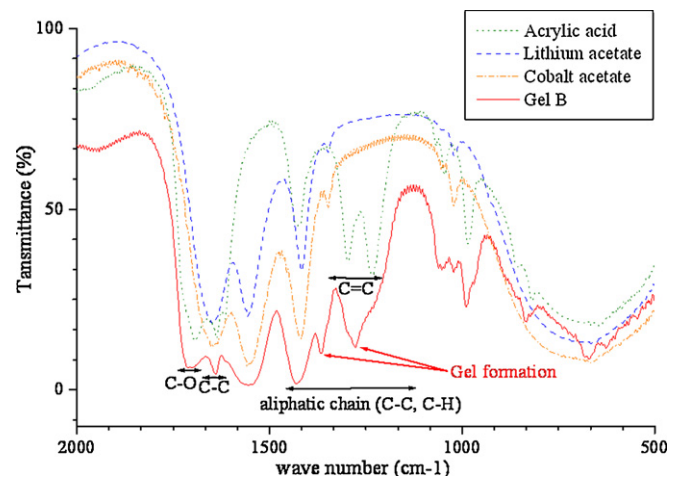


Fig. 6. IR spectra of precursors and gel B.



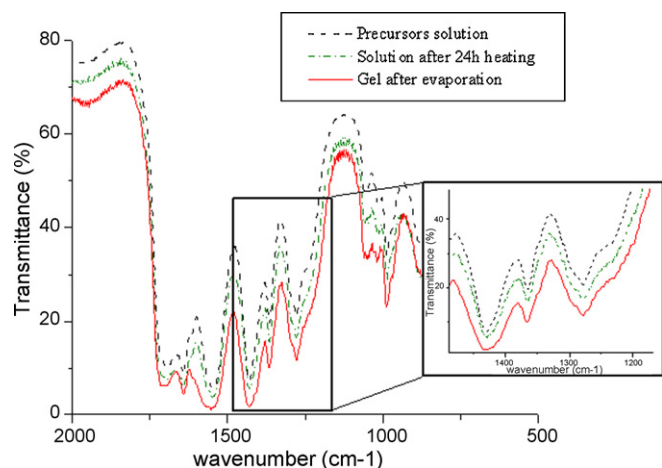


Fig. 7. IR spectra of gel B at different steps of the process.

this solvent (about  $20 \times 10^{-3} \text{ Pa s}^{-1}$ ) compared to water viscosity (about  $1.10^{-3} \text{ Pa s}^{-1}$ ). Moreover, it will be interesting in the case of multi-layers film to have gels with low viscosity to realize thinner deposit and it seems to be difficult with ethylene glycol solvent.

The affinity of the two solvents with the gold surface on the Au/TiO<sub>2</sub>/SiN/SiO<sub>2</sub>/Si substrate was determined by contact angle measurements (Fig. 9). Results show that wettability on the substrate is better with ethylene glycol ( $53.6 \pm 0.56^\circ$ ) than water ( $76.0 \pm 0.80^\circ$ ). As a consequence, the dewetting phenomenon is limited with ethylene glycol solvent during the gel spreading with the spin-coater.

Thermo Gravimetric Analyses of precursors and the resulting gel B are presented in Fig. 10. The weight loss begins at 60 °C with the decomposition of acrylic acid and the evaporation of adsorbed water. The decomposition of acetates occurs above 200 °C for cobalt salt and 330 °C for lithium salt. At 400 °C, all organic components are decomposed and the next weight loss occurs at 750 °C where the beginning of lithium evaporation is observed. Hence, the heat treatment for monolayer deposit was chosen to be a very low ramping until 400 °C to minimize the effect of organic component decomposition on thin film morphology followed by a dwell at 800 °C during 5 h, a particular attention was paid to lithium loss above 750 °C. Multilayers thin films were calcined at 400 °C between each deposit in order to decompose organic components deposit by deposit. R-3m LiCoO<sub>2</sub> was obtained by a final annealing at 800 °C.

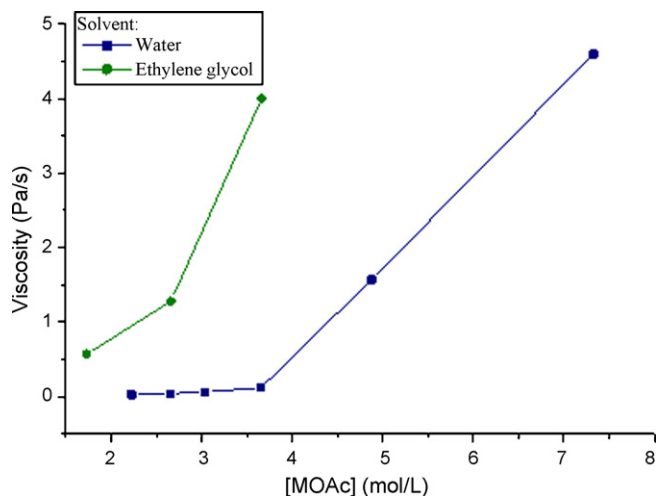


Fig. 8. Viscosity evolution with variation of concentration in different solvents.

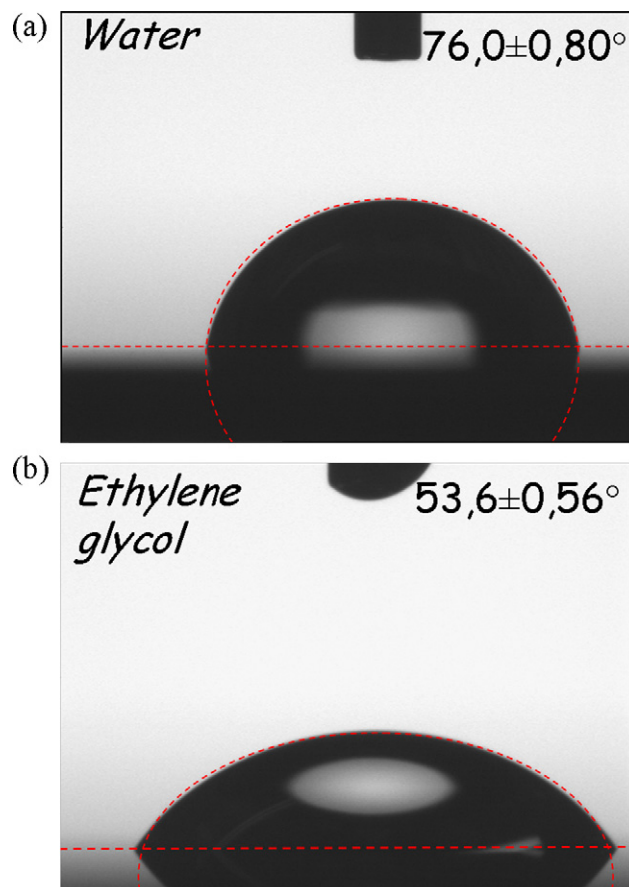


Fig. 9. Contact angle measurements of water and ethylene glycol on Au/Ti/SiN<sub>x</sub>/SiO<sub>2</sub>/Si substrate.

The deposition of thin films was realized by spin-coating with gel A or B. First tests were realized by depositing only one layer (Fig. 11). A delamination of the film from the substrate is observed mainly with high thicknesses due to the difference of thermal expansion coefficients between the film and the substrate. The film density was determined by a comparison between expected thickness based on the theoretical density of LiCoO<sub>2</sub> ( $5.06 \text{ g cm}^{-3}$ ),

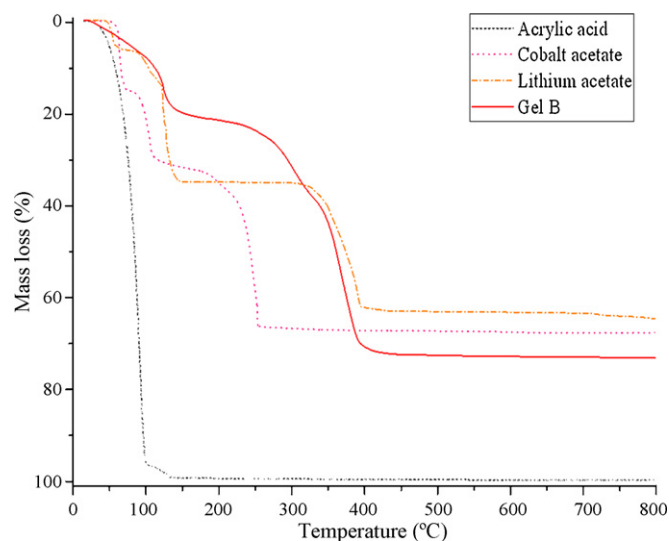
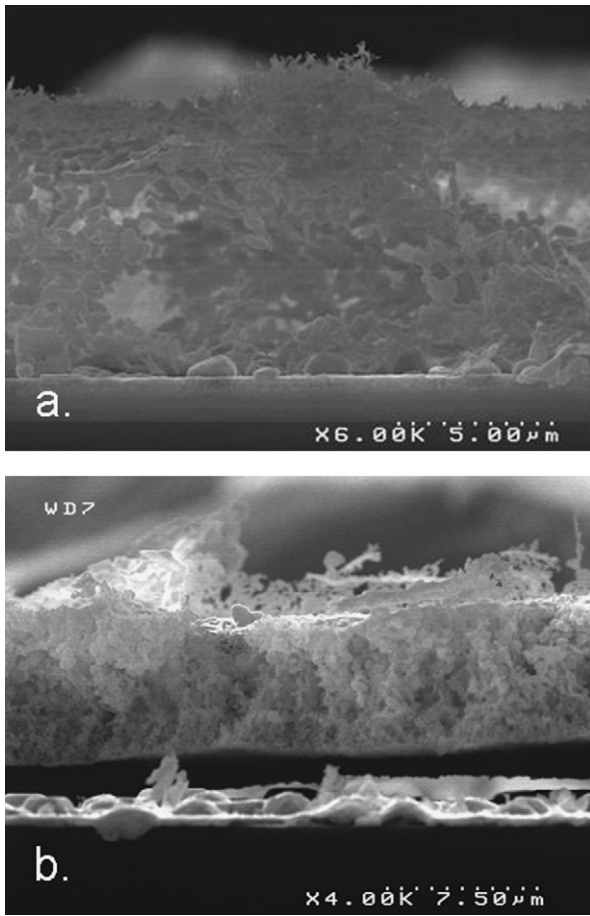


Fig. 10. TG analyses of precursors and gel B (heating rate of  $0.5^\circ \text{ mn}^{-1}$  from 25 to 450 °C and  $3^\circ \text{ mn}^{-1}$  until 800 °C).



**Fig. 11.** SEM cross-section views of single layer deposit with different solvent, (a) gel B ( $\eta = 118$  cP, 6000 $\times$ ), (b) gel A ( $\eta = 4000$  cP, 4000 $\times$ ).

**Table 2**  
Porosity of different deposits.

Gel	Viscosity (cP)	Layer(s)	Deposit porosity (%)
B	118	1	88
A	4000	1	84
B	63	6	56

the actual thickness of the deposit measured on SEM images and the mass of the deposited film. Calculations show that films have porosity above 85% (Table 2). This porosity is formed during the evacuation of gases resulting from the organic components decomposition. Multilayers deposits were realized to decompose gradually the organic components in order to limit the formation of porosity. Therefore, gel B with little evaporation rate and thus low viscosity was chosen to deposit low thickness films. Six layers were realized by spin-coating with the same conditions as described above (Fig. 12). Thickness measurements and porosity calculation on multilayers deposits show that film density is increased by 65% compared with monolayer films (Table 2). Delamination of the deposit is also observed for multilayers films. This phenomenon could be limited by lowering the temperature of the heat treatment taking into account the minimum temperature required to form R-3m phase.

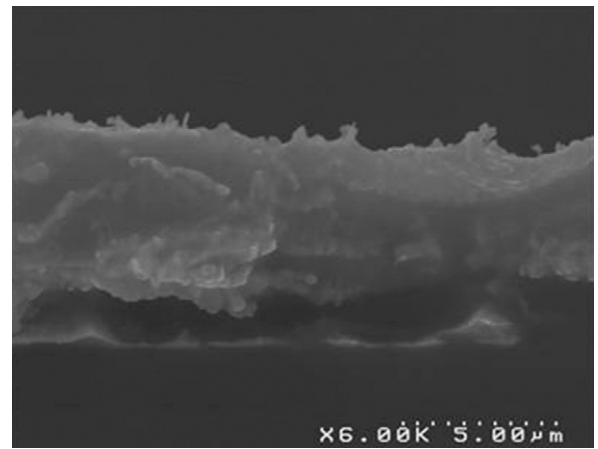


**Fig. 12.** SEM cross-section view of multilayers deposit (gel B (63 cP), 6000 $\times$ ).

#### 4. Conclusions

LiCoO<sub>2</sub> thin films were synthesized by coupling sol-gel process and spin-coating deposition. This work allowed optimizing the starting gel formulation and the profile of its thermal annealing. Infrared spectra confirm that acrylic acid acted as a chelating agent forming the gel as soon as it is present in the solution without requiring any heating. X-ray patterns show that LiCoO<sub>2</sub> R-3m phase is obtained with heat treatment at 800 °C. This result was confirmed by electrochemical analyses on coin cells.

Optimal formulation at this heat treatment temperature is molar ratios Li:Co of 1.02:1 and M<sup>+</sup>:AA of 1:1. Ideal solvent depends on the type of deposit. Because of its better wettability, ethylene glycol was the best solvent for monolayer deposit allowing higher thickness deposition. Water solvent was employed to deposit multilayers films which lead to higher density.

Delamination phenomenon occurs for every deposit. More tests have to be done to minimize film separation from the substrate, as explained above, by lowering heat treatment temperature or depositing a “buffer layer” between the film and the substrate in order to minimize the stress induced by heat treatment.

#### References

- [1] K. Mizushima, et al., *Materials Research Bulletin* 15 (6) (1980) 783–789.
- [2] J.N. Reimers, J.R. Dahn, *Journal of the Electrochemical Society* 139 (8) (1992) 2091–2097.
- [3] B. Garcia, et al., *Journal of the Electrochemical Society* 144 (4) (1997) 1179–1184.
- [4] M. Inaba, et al., *Journal of Raman Spectroscopy* 28 (8) (1997) 613–617.
- [5] G. Wei, T.E. Haas, R.B. Goldner, *Solid State Ionics* 58 (1–2) (1992) 115–122.
- [6] B. Wang, et al., *Journal of the Electrochemical Society* 143 (10) (1996) 3203–3213.
- [7] Y.K. Sun, I.H. Oh, S.A. Hong, *Journal of Materials Science* 31 (14) (1996) 3617–3621.
- [8] W.-S. Yoon, K.-B. Kim, *Journal of Power Sources* 81–82 (1999) 517–523.
- [9] M.Y. Song, R. Lee, *Journal of Power Sources* 111 (1) (2002) 97–103.
- [10] F.T. Quinlan, et al., *Industrial & Engineering Chemistry Research* 43 (10) (2004) 2468–2477.
- [11] M.-K. Kim, et al., *Journal of Power Sources* 99 (1–2) (2001) 34–40.
- [12] M.-K. Kim, et al., *Solid State Ionics* 152–153 (2002) 267–272.
- [13] Y.H. Rho, K. Kanamura, T. Umegaki, *Journal of the Electrochemical Society* 150 (1) (2003) A107–A111.
- [14] C.-T. Ni, K.-Z. Fung, *Solid State Ionics* 179 (21–26) (2008) 1230–1233.
- [15] J.N. Reimers, J.R. Dahn, U. Vonsacken, *Journal of the Electrochemical Society* 140 (10) (1993) 2752–2754.